arXiv:cond-mat/9606040v1 7 Jun 1996

Defect–induced condensation and central peak at elastic phase transitions

M. Bulenda, F. Schwabl, and U.C. Täuber *
Institut für Theoretische Physik,
Physik–Department der Technischen Universität München,
James–Franck–Straße, D–85747 Garching, Germany
(January 9, 2014)

Static and dynamical properties of elastic phase transitions under the influence of short–range defects, which locally increase the transition temperature, are investigated. Our approach is based on a Ginzburg–Landau theory for three–dimensional crystals with one–, two– or three–dimensional soft sectors, respectively. Systems with a finite concentration $n_{\rm D}$ of quenched, randomly placed defects display a phase transition at a temperature $T_c(n_{\rm D})$, which can be considerably above the transition temperature T_c^0 of the pure system. The phonon correlation function is calculated in single–site approximation. For $T > T_c(n_{\rm D})$ a dynamical central peak appears; upon approaching $T_c(n_{\rm D})$, its height diverges and its width vanishes. Using an appropriate self–consistent method, we calculate the spatially inhomogeneous order parameter, the free energy and the specific heat, as well as the dynamical correlation function in the ordered phase. The dynamical central peak disappears again as the temperatur is lowered below $T_c(n_{\rm D})$. The inhomogeneous order parameter causes a static central peak in the scattering cross section, with a finite k width depending on the orientation of the external wave vector $\mathbf{k}$ relative to the soft sector. The jump in the specific heat at the transition temperatur of the pure system is smeared out by the influence of the defects, leading to a distinct maximum instead. In addition, there emerges a tiny discontinuity of the specific heat at $T_c(n_{\rm D})$. We also discuss the range of validity of the mean–field approach, and provide a more realistic estimate for the transition temperature.

PACS numbers: 64.60.-i, 61.72.-y, 63.20.Mt, 64.60.Ht

I. INTRODUCTION

The influence of defects on the statics and dynamics of structural phase transitions has been of considerable theoretical interest over the past two decades [1–8]. Especially the appearence of a narrow central peak in the neutron scattering cross section, well above the transition temperature, for both distortive [9] and elastic structural transitions [10], prompted various theoretical studies dealing with local ordering phenomena around short–range static defects (for a review of the experimental facts, see Ref. [11] and Ref. [12], and for a review of some theoretical results, see Ref. [13]).

E.g., in Ref. [3] a one–dimensional model for continuous distortive structural transitions was studied, with the order parameter coupling to a single defect ($N_{\rm D} = 1$). If the impurity locally increases the transition temperature T_c^0 of the pure system, this leads to a local condensation of the order parameter in the defect vicinity. In higher dimensions, for this local order parameter condensation to occur, the defect potential strength must exceed a certain minimal threshold. Such locally ordered regions in the material emerging well above the pure transition temperature T_c^0 have played a prominent role in some of the theories attempting to explain the central peak phenomenon for distortive and elastic structural phase transitions [1–6]. In this paper, we extend previous work on second–order ferroelastic phase transitions in $d = 1$ [7] to higher space dimensions d, taking into account the crystalline anisotropy. To this end, we shall generalize the methods developed for the distortive case [8] to (anisotropic) elastic systems, thus treating consistently a random impurity system with finite defect concentration $n_{\rm D}$ (in the thermodynamic limit, both the number of lattice sites $N \to \infty$ and the number of defects $N_{\rm D} \to \infty$, but $n_{\rm D} = N_{\rm D}/N = \text{const.}$).

In the framework of our mean–field approach, we shall find that defects which locally soften the crystal may induce a true phase transition at a temperature $T_c(n_{\rm D}) > T_c^0$. Below this defect–induced phase transition temperature a spatially inhomogeneous order parameter emerges, whose average value remains very small in the vicinity of $T_c(n_{\rm D})$ and only becomes noticeable near T_c^0. Similarly, thermodynamic quantities (static susceptibility, specific heat, etc.) display prominent, broadened maxima near T_c^0 suggesting a "rounded" phase transition; however, the "true" singularities occur at $T_c(n_{\rm D})$, but may not be seen in experiment at all, as their amplitude is only proportional to the defect concentration $n_{\rm D}$. The Bragg peaks of the low–temperature phase already appear in the scattering cross section for $T < T_c(n_{\rm D})$; as a consequence of the spatial inhomogeneity of the order parameter, they are accompanied by elastic Huang scattering peaks with finite q width. Furthermore, very close to $T_c(n_{\rm D})$ an ad-

ditional dynamic central peak emerges, which may be interpreted as a dynamical precursor to the defect–induced phase transition.

These mean–field results of course neglect order parameter fluctuations, and exaggerate cooperative behavior. In reality, at $T \approx T_c(n_{\rm D})$ localized order parameter clusters appear, whose orientations however strongly fluctuate in space. Only at a lower temperature $T_{\rm ord} < T_c(n_{\rm D})$ (if at all) will they form a collective state with uniform orientation, i.e.: the spatially inhomogeneous configuration predicted by mean–field theory. In order to provide a more realistic estimate of the proposed defect–induced transition temperature, we consider the cluster orientations as effectively Ising–like degrees of freedom, and then determine the cluster ordering temperature $T_{\rm ord}$ by calculating the free–energy difference of states with parallel and opposite orientation, respectively. Thus the onset of the order parameter, the Bragg peaks, and the Huang scattering will be shifted to somewhat lower temperatures, and the results of this work can essentially be used if $T_c(n_{\rm D})$ is replaced by $T_{\rm ord}$. Provided that $T_{\rm ord}$ is still considerably larger than T_c^0, we thus expect the behavior of the thermodynamic quantities near T_c^0 to be very similar to the results presented here.

This paper is organized as follows: In Sec. II we introduce the Ginzburg–Landau functional for a d–dimensional system, with one m–dimensional soft sector, including randomly distributed point defects. The corresponding Langevin–type equation of motion is formulated. Furthermore we present an expression for the density–density correlation function, which serves as a starting point for subsequent considerations. In Sec. III the phonon response function is evaluated in the high–temperature phase, and the emergence of a dynamical central peak and a defect–induced phase transition well above T_c^0 is demonstrated. In Sec. IV we proceed to the ordered low–temperature phase, by using a suitable self–consistent approach. We determine the spatially inhomogeneous order parameter, the free energy and specific heat, as well as the phonon correlation function, and discuss the singularities in these quantities. In addition, the scattering cross section $S(\mathbf{k})$ (i.e., the density–density correlation function) is studied. In Sec. V we leave the realm of mean–field theory, and provide an estimate of the "true" defect–induced transition temperature (for the isotropic case), by identifying it with that temperature where already existing, but still fluctuating clusters condense to form a non–zero average order parameter. In Sec. VI, we briefly discuss the case of extended disorder (line or planar defects), and in Sec. VII we finally summarize and discuss our results.

II. GENERAL EQUATIONS

A. Model

In order to describe elastic phase transitions of second order in d dimensions with an m–dimensional soft sector, we use an expansion of the elastic free energy of the unperturbed crystal with respect to phonon normal coordinates $Q_{\mathbf{k}}$, [14,15]. We disregard non–critical polarizations; furthermore, aiming at the long–wavelength limit we keep only the lowest–order terms in the wavevector expansion of the dispersion relation of the acoustic phonons. The wavevector $\mathbf{k}$ is then decomposed into its m–dimensional "soft" components $\mathbf{p}$, and its $(d-m)$–dimensional "stiff" part $\mathbf{q}$, respectively: $\mathbf{k} = (\mathbf{p}, \mathbf{q})$. Folk, Iro, and Schwabl have shown that terms of the form q^4 or q^2p^2 are irrelevant (in the renormalization group sense) and do not affect the critical behavior of the system [14]. In this spirit we use the following effective free energy

$$F = \int d^dk \int d^dk' \frac{1}{2} \left[\left(ap^2 + bq^2 + cp^4 \right) \delta(\mathbf{k} - \mathbf{k}') Q_{\mathbf{k}} Q_{-\mathbf{k}'} \right] + \mathcal{O}(Q_{\mathbf{k}}^4) \ . \tag{2.1}$$

The coefficient a is assumed to depend linearly on temperature, vanishing at T_c^0: $a = a'(T - T_c^0)$; the very weak temperature dependence of the Ginzburg–Landau coefficients b and c is neglected.

In order to describe the influence of short–range defects, which locally increase the transition temperature, we assume that each defect creates a short–range potential at its site, thus locally modifying the coefficients a and b of the Ginzburg–Landau functional (2.1); being interested in long–wavelength properties of the system, we can thus model the defect potential in the continuum by a δ function. The coefficient a will be particularly sensitive to such a modification, as it becomes very small near the transition. For the coefficient c and the higher–order coefficients the defect influence is less important and will be neglected. We thus arrive at the following Ginzburg–Landau functional for the perturbed system,

$$F = \int d^dk \int d^dk' \frac{1}{2} \left[\left(ap^2 + bq^2 + cp^4 \right) \delta(\mathbf{k} - \mathbf{k}') Q_{\mathbf{k}} Q_{-\mathbf{k}'} - \phi_{\mathbf{k},\mathbf{k}'} \mathbf{k}\mathbf{k}' Q_{\mathbf{k}} Q_{-\mathbf{k}'} \right] + \mathcal{O}(Q_{\mathbf{k}}^4) \ , \tag{2.2}$$

where $\phi_{\mathbf{k},\mathbf{k}'}$ denotes the Fourier transform of the impurity potential (created by $N_{\rm D}$ defects)

$$\phi(\mathbf{r}) = U \sum_{i_{\rm D}=1}^{N_{\rm D}} \delta(\mathbf{r} - \mathbf{r}_{i_{\rm D}}) \ . \tag{2.3}$$

The defect strength $U = a_0^d \lambda$ is taken to be positive, and therefore the transition temperature is locally increased at the impurities (here, V is the volume of the system, and $a_0^d = V/N$ denotes the volume of the unit cell).

The dynamics of the elastic crystal are governed by a Langevin–type equation of motion for the soft acoustic phonons [16],

$$M\omega^2 Q_{\mathbf{k}} = -\frac{\delta F}{\delta Q_{-\mathbf{k}}} - iM\omega(Dp^2 + \tilde{D}q^2)Q_{\mathbf{k}} + r_{\mathbf{k}} + h_{\mathbf{k}} \ . \tag{2.4}$$

The term on the left–hand side of Eq.(2.4) describes the acceleration, while the first term on the right–hand side provides the restoring force driving the system towards its equilibrium configuration. Note that we have introduced two different diffusive damping constants D and $\tilde{D}$ for the soft and stiff sectors, respectively. $r_{\mathbf{k}}$ denotes a stochastic force with vanishing average, $\langle r_{\mathbf{k}} \rangle = 0$; its second moment satisfies an Einstein relation, guaranteeing that $\exp(-F/k_{\rm B}T)$ is the equilibrium probability distribution. Finally, h is an external field which couples linearly to the order parameter. Eq.(2.4) will be the basis for our discussion of the dynamical properties in the subsequent chapters.

B. Density–density correlation function

In the following we shall primarily use a discrete lattice representation of the elastic system under consideration. The dynamic structure factor observed in scattering experiments is related to the Fourier–transformed density–density correlation function. Denoting the thermodynamical average by $\langle \ldots \rangle$, its definition is

$$S(\mathbf{k},\omega) = \int dt e^{i\omega t} \left\langle \frac{1}{N} \sum_{1 \le i,j \le N} e^{-i\mathbf{k}[\mathbf{a}_i + \mathbf{u}_i(t)]} e^{i\mathbf{k}[\mathbf{a}_j + \mathbf{u}_j(0)]} \right\rangle \ , \tag{2.5}$$

where $\mathbf{a}_i$ denote the Bravais lattice sites (of the high–temperature phase), and $\mathbf{u}_i$ the displacements from these equilibrium positions.

In the discrete representation, with N lattice sites, we can write the Fourier–transformed defect potential as

$$\phi_{\mathbf{k}\mathbf{k}'} = \frac{1}{N} \sum_{i,j=1}^{N} \left(\sum_{i_{\rm D}=1}^{N_{\rm D}} \lambda \delta_{i,i_{\rm D}} \delta_{ij} \right) e^{-i(\mathbf{k}\mathbf{x}_i - \mathbf{k}'\mathbf{x}_j)} \ . \tag{2.6}$$

In a system with quenched, randomly distributed defects, all physical quantities have to be averaged over all possible defect configurations [17]. We denote this configurational average by $\langle\langle \ldots \rangle\rangle$; its formal definition reads

$$\langle\langle \ldots \rangle\rangle = \prod_{j=1}^{N_{\rm D}} \left[\frac{1}{N} \sum_{i_{{\rm D}_j}}^{N} \right] \ldots \ . \tag{2.7}$$

In order to evaluate $\langle\langle S(\mathbf{k},\omega)\rangle\rangle$, we introduce a cumulant expansion for the combined thermal and configurational averages of $e^{i\mathbf{k}[\mathbf{u}_j(0) - \mathbf{u}_i(t)]}$ and keep the terms up to second order. Next we decompose the deviations $\mathbf{u}_i(t)$ into a static contribution ψ_i and a fluctuating part $\mathbf{v}_i(t)$, and expand the exponential. Eventually one arrives at the following formula for the dynamical structure factor (for more details on the derivation, see Ref. [8])

$$\langle\langle S(\mathbf{k},\omega)\rangle\rangle = \left[N \sum_{\mathbf{g}} \delta_{\mathbf{k},\mathbf{g}} + \sum_{\alpha\beta} k^\alpha k^\beta \langle\langle S_c^{\alpha\beta}(\mathbf{k})\rangle\rangle \right] \times e^{-2W} 2\pi\delta(\omega) + \left[\sum_{\alpha\beta} k^\alpha k^\beta D^{\alpha\beta}(\mathbf{k},\omega) \right] e^{-2W} \ . \tag{2.8}$$

The three different contributions to the dynamical structure factor in Eq.(2.8) are (i) the elastic Bragg peaks appearing at the reciprocal lattice vectors $\mathbf{g}$ of the actual crystal structure, given by the condition

$$e^{i\mathbf{g}\left(\mathbf{a}_i + \langle\langle \psi_i \rangle\rangle\right)} = 1 \ ; \tag{2.9}$$

(ii) an additional static contribution to the structure factor arising from elastic scattering from the random variations of the local order parameter (Huang scattering)

$$S_c^{\alpha\beta}(\mathbf{k}) = \frac{1}{N} \sum_{i,j} e^{-i\mathbf{k}(\mathbf{a}_i - \mathbf{a}_j)} \left(\psi_i^\alpha \psi_j^\beta - \langle\langle \psi_i^\alpha \rangle\rangle \langle\langle \psi_j^\beta \rangle\rangle \right) \ ; \tag{2.10}$$

and (iii) the dynamical phonon–phonon correlation function

$$D^{\alpha\beta}(\mathbf{k},\omega) = \int dt e^{i\omega t} \left\langle \left\langle \frac{1}{N} \sum_{i,j} e^{-i\mathbf{k}(\mathbf{a}_i - \mathbf{a}_j)} \langle v_i^\alpha(t) v_j^\beta(0) \rangle \right\rangle \right\rangle \ , \tag{2.11}$$

which is connected with the dynamic phonon response function via the (classical) fluctuation–dissipation theorem

$$D^{\alpha\beta}(\mathbf{k},\omega) = \frac{2k_{\rm B}T}{\omega} {\rm Im}\ G^{\alpha\beta}(\mathbf{k},\omega) \ . \tag{2.12}$$

Finally,

$$W = \frac{1}{2} \sum_{\alpha\beta} k^\alpha k^\beta \left[\left\langle \left\langle \left(\psi_i^\alpha - \langle\langle \psi_i^\alpha \rangle\rangle \right) \left(\psi_i^\beta - \langle\langle \psi_i^\beta \rangle\rangle \right) \right\rangle \right\rangle + \left\langle \left\langle \langle v_i^\alpha v_i^\beta \rangle \right\rangle \right\rangle \right] \tag{2.13}$$

is the Debye–Waller factor. Eq.(2.8) may be used for elastic as well as for distortive phase transitions. For antiferrodistortive transitions one has to sum over the distinct sublattices in addition (see Ref. [8]). The dynamic phonon–phonon correlation function (2.11) and the static Huang scattering contribution (2.10) will be discussed in more detail below.

III. HIGH–TEMPERATURE PHASE

In order to calculate the phonon correlation function in the high temperature phase, Eq.(2.2) is inserted in the equation of motion (2.4). Note that nonlinearities in the phonon normal coordinates are neglected, and thus fluctuations are only being accounted for in the Gaussian approximation. Upon differentiating the resulting expression with respect to $h_{\mathbf{k}'}$, and transcribing it to the corresponding discrete version, and finally using the fact that the average of the stochastic force $r_{\mathbf{k}'}$ vanishes, one arrives at the following mean–field recursion relation for the phonon response function

$$G_{\mathbf{k}\mathbf{k}'} = G_{0\mathbf{k}}\delta_{\mathbf{k}\mathbf{k}'} + G_{0\mathbf{k}} \sum_{\mathbf{k}''} \phi_{\mathbf{k}\mathbf{k}''}\mathbf{k}\mathbf{k}''G_{\mathbf{k}''\mathbf{k}'} \ , \tag{3.1}$$

with the free phonon propagator

$$G_{0\mathbf{k}}^{-1} = -M\omega^2 + ap^2 + bq^2 + cp^4 - iM\omega(Dp^2 + \tilde{D}q^2) \ . \tag{3.2}$$

Eq.(3.1) may then be systematically iterated, and the configurational average (2.7) performed; e.g., applying a standard diagrammatic technique helps in collecting all the contributions to a certain order in the defect potential strength λ [17,18]. The configurational average yields a translationally invariant response function,

$$\langle\langle G_{\mathbf{k}\mathbf{k}'}\rangle\rangle = G_{\mathbf{k}}\delta_{\mathbf{k}\mathbf{k}'} \ . \tag{3.3}$$

Upon collecting all contributions which are proportional to the impurity concentration $n_{\rm D} = N_{\rm D}/N$ (single–site approximation; for more details, see Ref. [8]), the result for the phonon susceptibility is

$$G_{\mathbf{k}}^{-1} = -M\omega^2 + ap^2 + bq^2 + cp^4 - iM\omega(Dp^2 + \tilde{D}q^2) - \frac{\lambda k^2 n_{\rm D}}{1 - \lambda(a_0/2\pi)^d I_d(m)} \ . \tag{3.4}$$

Here we have introduced the abbreviation

$$\begin{aligned} I_d(m) &= \int_0^\Lambda \frac{(p^2+q^2)}{-M\omega^2 + ap^2 + bq^2 + cp^4 - iM\omega(Dp^2+\tilde{D}q^2)} d^m p \ d^{d-m}q \\ &= m(d-m)\tau_m\tau_{d-m}\int_0^\Lambda \frac{(p^2+q^2)p^{m-1}q^{d-m-1}}{-M\omega^2 + ap^2 + bq^2 + cp^4 - iM\omega(Dp^2+\tilde{D}q^2)} dp \ dq \ , \end{aligned} \tag{3.5}$$

and τ_n is the volume of the n–dimensional unit sphere

$$\tau_n = \frac{\pi^{n/2}}{\Gamma\left(\frac{n}{2}+1\right)} \ . \tag{3.6}$$

Λ denotes a natural short–wavelength cutoff (e.g., corresponding to the Brillouin zone boundary), which also helps to ensure the convergence of the integral $I_d(m)$. Note that the dimension m of the soft sector in k space explicitly enters in Eq.(3.5), and thus determines the importance of the fluctuation contributions.

Eq.(3.4) implies the very remarkable result that due to the coupling to the softening defects, the entire system may become unstable towards a new ground state with finite average order parameter at a certain temperature $T_c(n_{\rm D})$, depending on the defect concentration $n_{\rm D}$; the criterion for this instability is

$$\lim_{k\to 0}\left[G_{\mathbf{k}}^{-1}(\omega=0)/k^2\right] = 0 \ . \tag{3.7}$$

As in the distortive case [8], we find that in general a certain minimal defect strength is required for this instability to occur; yet, once this defect–induced phase transition does exist, the associated transition temperature $T_c(n_{\rm D})$ can be considerably higher than that of the pure system, T_c^0. (In Sec. V, we shall comment on the validity of the mean–field approach, and estimate the transition temperature on a more realistic basis.)

We have investigated three–dimensional systems with one one–, two– or three–dimensional soft sector, respectively. The qualitative features were found to be very similar in all these cases. The following figures refer to a three–dimensional system with a single one–dimensional soft sector. We have tried to use model parameters appropriate for Nb_3Sn, which displays a second–order elastic phase transition near $T = 45$K [20]; accordingly, we have used numerical values calculated from Refs. [19,20] (Table I). Thus, we have taken $T_c^0 = 45$K, $n_{\rm D} = 10^{-5}$, and adjusted the defect strength in order that $T_c(n_{\rm D}) = 65K$. However, a few remarks are in place here to explain some sources of inaccuracies. The assumption that the Ginzburg–Landau parameter a is merely linearly temperature–dependent is valid only near the phase transition temperature of the pure system T_c^0. Furthermore we approximated c and b as independent of temperature, and in addition assumed b to be independent of the direction of the $\mathbf{k}$ vector in the stiff plane. This is not generally the case for Nb_3Sn, but appears to describe the critical region well. The numerical values of the diffusion constant $D = \tilde{D}$ and the nonlinearity d (see below) had to be estimated without reference to any experiment.

Fig.1 depicts the phonon correlation function $D(\mathbf{k},\omega)$ [Eq.(2.12)] for different temperatures $T > T_c(n_{\rm D})$, evaluated for several angles θ between the external wave vector and the soft sector. As becomes apparent in Fig.1, a dynamical central peak in the phonon correlation function emerges in addition to the soft phonon peak (compare Ref. [7] for the one–dimensional case). The height of the central peak grows, and its width decreases as $T_c(n_{\rm D})$ is approached. The intensity of the central peak decreases

upon increasing the angle θ between the wave vector $\mathbf{k}$ and the soft sector. This reflects the fact that wavevectors in the stiff sector do not probe the critical properties of the material. The dynamical central peak may thus be understood as a dynamic precursor to the defect–induced second–order phase transition at $T_c(n_{\rm D})$.

IV. LOW–TEMPERATURE PHASE

In this section, we use a self–consistent approach designed for the calculation of the order parameter ν, the specific heat, the phonon correlation function and finally the dynamical structure factor in the ordered phase, i.e., for $T < T_c(n_{\rm D})$.

A. Order parameter

The starting point for the calculation of the order parameter is the full nonlinear Ginzburg–Landau functional, which in the discrete lattice representation reads

$$F = \frac{1}{2}\sum_{i,j=1}^{N} \nu_i G_{0ij}^{-1} \nu_j - \frac{\lambda}{2}\sum_{i=1}^{N}\sum_{i_{\rm D}=1}^{N_{\rm D}} \nu_i^2 \delta_{ii_{\rm D}} + \frac{d}{4}\sum_{i=1}^{N}\nu_i^4 - \sum_{i=1}^{N} h_i \nu_i \ . \tag{4.1}$$

Here ν_i denotes the value at lattice site i of that combination of strain tensor components serving as the order parameter for the transition, h_i is the corresponding external stress acting on site i, and the static propagator G_{0ij} is defined by its Fourier transform

$$\begin{aligned} G_{0\mathbf{k}}^{-1} &= a + ck^2 \quad \text{for } d = m, \\ G_{0\mathbf{k}}^{-1} &= \frac{ap^2 + bq^2 + cp^4}{k^2} \quad \text{for } d > m. \end{aligned} \tag{4.2}$$

In the framework of the Ginzburg–Landau approximation, i.e., neglecting order parameter fluctuations, the following stationarity condition can be derived (with $h_i = h = \text{const.}$)

$$\frac{\delta F}{\delta \nu_i} = 0 \quad \Leftrightarrow \quad \sum_j G_{0ij}^{-1}\nu_j - \lambda \sum_{i_{\rm D}} \nu_i \delta_{i,i_{\rm D}} + d\nu_i^3 = h \ . \tag{4.3}$$

A general solution of Eq.(4.3), with its combined nonlinearity and randomness, poses a difficult problem. We thus use an additional approximation, namely the following ansatz [8] for the thermodynamical average of the order parameter (denoted by $\bar{\nu}$),

$$\bar{\nu}_i = A + B\sum_{i_{\rm D}} \delta_{i,i_{\rm D}} \ , \tag{4.4}$$

i.e.: we assume that the order parameter at each lattice point i may be written as the sum of a homogeneous background A and an additional contribution B, if there is a defect at site i, thus enhancing the total value of the order parameter to $A+B$ at the defect sites. Thus we explicitly assume that at all defect sites the order parameter points in the same direction, and in addition neglect the spatial variation of the order parameter near the defects. However, as we shall see shortly, the second, seemingly very crude approximation already contains the possible relevant modifications caused by the impurities, namely (i) an enhancement of the spatially averaged order parameter (corresponding to the parameter A), and (ii) the ensuing "screening" of the defect potential (described by the coefficient B). The more stringent approximation is the uniform orientation of the defect clusters, as implied by the mean–field approach (see Sec. V).

Inserting Eq. (4.4) into the stationarity equation (4.3) yields the recursion relation

$$\bar{\nu}_{\mathbf{k}} = h\delta_{\mathbf{k}0}\tilde{G}_0(\mathbf{k}) + \tilde{G}_0(\mathbf{k})\sum_{\mathbf{k}'} \tilde{\phi}_{\mathbf{k}\mathbf{k}'}\bar{\nu}_{\mathbf{k}'} \ , \tag{4.5}$$

where we have introduced a renormalized propagator

$$\tilde{G}_0(\mathbf{k})^{-1} = G_0(\mathbf{k})^{-1} + dA^2 \ , \tag{4.6}$$

and a screened defect potential $\tilde{\phi}_{\mathbf{k}\mathbf{k}'}$ with weakened strength [see Eq.(2.6)]

$$\tilde{\lambda} = \lambda - d[(A+B)^2 - A^2] \ . \tag{4.7}$$

From Eq.(4.5) and the averaged stationarity equation we may derive two coupled nonlinear equations that uniquely determine the mean order parameter: (i) Iterating the recursion relation (4.5) in a similar way as for the dynamics in the previous paragraph, performing the configurational average, and summing the single–site contributions, one arrives at

$$\frac{\langle\langle\bar{\nu}\rangle\rangle}{h} = \left[a + dA^2 - \frac{\tilde{\lambda} n_{\rm D}}{1 - \tilde{\lambda}(a_0/2\pi)^d J_d}\right]^{-1} \ , \tag{4.8}$$

with the abbreviation

$$J_d = \int d^d k \frac{k^2}{(a+dA^2)p^2 + (b+dA^2)q^2 + cp^4} \ . \tag{4.9}$$

(ii) On the other hand, immediate averaging of Eq.(4.5) yields

$$(a + dA^2)(A + n_{\rm D}B) - \tilde{\lambda} n_{\rm D}(A+B) - h = 0 \ . \tag{4.10}$$

Very assuringly, Eqs.(4.8) and (4.10) yield non–zero solutions for $\langle\langle\bar{\nu}\rangle\rangle$ precisely below $T_c(n_{\rm D})$ as determined from the high–temperature phase. Fig.2 shows that the order parameter of the perturbed system as function of T looks similar to the corresponding curve for the pure system,

with the singularity at T_c^0 being smeared out by the disorder. The order parameter sets in continuously at $T_c(n_{\rm D})$, with the usual mean–field exponent $\beta = 1/2$, assumes small but finite values in the range $T_c(n_{\rm D}) > T > T_c^0$, and starts to grow to larger values only in the vicinity of T_c^0. Thus the transition temperature of the pure system remains an important parameter even in the perturbed system, while the true phase transition at $T_c(n_{\rm D})$ may in fact be hardly noticeable in experiments. As before, the results for a three–dimensional system with one one–dimensional soft sector are depicted, but the qualitative features remain essentially the same in the cases of a two– or three–dimensional soft sector.

B. Specific heat

From the knowledge of the mean order parameter, we can readily calculate the (averaged) free energy from Eq.(4.1) in Landau approximation, and via

$$C_v = -T \left(\frac{\partial^2 F}{\partial T^2} \right)_V \tag{4.11}$$

derive the specific heat C_v, see Fig.3. Obviously, the discontinuity at T_c^0 has been smeared out, in place of which a tiny jump emerges at $T_c(n_{\rm D})$. Although the phase transition clearly occurs at $T_c(n_{\rm D})$, the transition temperature T_c^0 of the pure system remains of considerable importance; e.g., there is a distinct maximum of the specific heat near T_c^0, while the extremely minute jump at $T_c(n_{\rm D})$ might not be experimentally detectable at all.

C. Phonon correlation function in the ordered phase

In order to find the phonon correlation function in the temperature region with a finite order parameter, one again has to start from the full Ginzburg–Landau functional and use the ansatz for the order parameter (4.4). The crucial point is that one may then absorb the nonlinear term of the equation of motion in modified coefficients of the linear terms as follows

$$a \to a + 3dA^2 \,, \quad b \to b + 3dA^2 \,, \quad \lambda \to \lambda - 3dB(2A + B). \tag{4.12}$$

With these modifications one can use the same equations as in the high–temperature phase.

The result is depicted in Fig.4. The central peak in the correlation function disappears again when the temperature is lowered below $T_c(n_{\rm D})$. This dynamical central peak is thus confined to the region around $T_c(n_{\rm D})$. As in the high–temperature phase, the intensity of the central peak decreases upon increasing the angle between the external $\mathbf{k}$ vector and the soft sector (with fixed temperature).

In Fig.5 the static phonon susceptibility $G(\mathbf{k}) = G_{\mathbf{k}}(\omega = 0)$ (i.e., the inverse elastic constant, as modified by the defects) is shown. The small but sharp peak at $T_c(n_{\rm D})$ reflects the preordering of the defect regions, while the broad and much more prominent peak near T_c^0 corresponds to the ordering of the pure bulk crystal, though under the influence of the randomly spaced fields originating from the defect clusters; compare Figs.2 and 3.

D. Dynamical structure factor

In order to describe scattering experiments, we have to calculate the density–density correlation function of Sec.2. The first term in Eq.(2.8) yields the Bragg scattering, and does not require any further comment; the third term is connected with the phonon correlation function, and has been discussed in the previous subsection. We therefore turn our attention to the second term. Taking into account the soft acoustic phonon mode only, as above, we have to calculate the configurational average of $k^2 \psi_{\mathbf{k}} \psi_{-\mathbf{k}}$ [Eq.(2.10)]; using the same approximations as in the beginning of Sec.3, we may use equation (4.5) in the form

$$k\psi_{\mathbf{k}} = h\tilde{G}_0(0)\delta_{\mathbf{k}0} + \tilde{G}_0(\mathbf{k}) \sum_{\mathbf{k}'} \tilde{\phi}_{\mathbf{k}\mathbf{k}'} \bar{\nu}_{\mathbf{k}'} \,, \tag{4.13}$$

which yields

$$k^2 \psi_{\mathbf{k}} \psi_{-\mathbf{k}} = h^2 \tilde{G}_0(0)^2 \delta_{\mathbf{k}0} + h\tilde{G}_0(0)^2 \sum_{\mathbf{k}'} \tilde{\phi}_{0\mathbf{k}'} \bar{\nu}_{\mathbf{k}'} \delta_{\mathbf{k}0} + \tilde{G}_0(\mathbf{k}) \sum_{\mathbf{k}'} \tilde{\phi}_{\mathbf{k}\mathbf{k}'} \bar{\nu}_{\mathbf{k}'} \bar{\nu}_{-\mathbf{k}} \,. \tag{4.14}$$

For this equation again a diagrammatic representation can be derived [8], and in single–site approximation (i.e.: to order $n_{\rm D}$) we find the following result ($\mathbf{k}_L$ denotes the components of the wave vector which are parallel to the polarization of the soft mode)

$$k^2 S_c^{LL}(\mathbf{k}) = n_{\rm D} \tilde{\lambda}^2 \langle\langle \bar{\nu} \rangle\rangle^2 (k^L)^2 \tilde{G}_0(\mathbf{k}) \tilde{G}_0(-\mathbf{k}) \times \left[1 - \frac{\tilde{\lambda}}{N} \sum_{k'} \tilde{G}_0(\mathbf{k}') \right]^{-2} \,. \tag{4.15}$$

This expression can be further reduced using Eq. (4.8). Finally, we arrive at

$$k^2 S_c^{LL}(\mathbf{k}) = (a + dA^2)^2 \frac{\langle\langle \nu \rangle\rangle^2}{n_{\rm D}} (k^L)^2 \tilde{G}_0(\mathbf{k})^2 \,. \tag{4.16}$$

Collecting all results, the final expression for the dynamical structure factor reads

$$\langle\langle S(\mathbf{k},\omega)\rangle\rangle = \left[N\sum_{\mathbf{g}} \delta_{\mathbf{g},\mathbf{k}} + \frac{(k^L)^2}{k^2}\frac{\langle\langle\bar{\nu}\rangle\rangle^2}{n_{\rm D}}\tilde{G}_0(\mathbf{k})^2(a+dA^2)^2 \right] e^{-2W} 2\pi\delta(\omega) + (k^L)^2 D(\mathbf{k},\omega) e^{-2W} \ . \tag{4.17}$$

Thus we have found three distinct effects, namely (i) new positions of the Bragg peaks as a result of the finite order parameter [shifted and possibly new reciprocal lattice vectors, see Eq.(2.9)] ; (ii) Huang scattering as a result of the spatially inhomogeneous order parameter configuration, leading to a static central peak with finite width $\gamma = \sqrt{(a+dA^2)/c}$ (in the soft sector) in Fourier space; and (iii) inelastic scattering, described by the phonon correlation function. Fig.6 shows how the intensity of the Huang scattering varies with temperature for different wave vectors $\mathbf{k} = \mathbf{p}$ in the soft sector. This additional elastic contribution sets in at $T_c(n_{\rm D})$, and then grows to considerable values near T_c^0.

V. ESTIMATE OF THE CLUSTER ORDERING TEMPERATURE

All our previous results for the statics were based entirely on the Ginzburg–Landau approximation, and dynamic quantities were calculated in the Gaussian ensemble. This mean–field treatment of course neglects fluctuations, and apart from the fact that the critical exponents will be changed near the transition, we have to consider the possibility that the above described defect–induced phase transition at $T_c(n_{\rm D})$ will disappear when fluctuations are properly taken into account. Namely, our mean–field approach basically implies that as soon as local condensates form near the defects, they immediately lock into some cooperative state and form a non–vanishing average order parameter. In reality, probably first these clusters may emerge at the defect positions, however still quite independently fluctuating between their different possible orientations. Only as the temperature is lowered even further, they will form a collective vibrational mode which finally condenses to a static order parameter at the "true" transition temperature $T_{\rm ord}$, with $T_c^0 \le T_{\rm ord} \le T_c(n_{\rm D})$, the mean–field transition temperature. One would expect that such collective behavior of the distinct localized order parameter clusters arises when the correlation length of the pure system ξ, which determines the size of the defect–induced condensates, becomes of the order of the average defect separation $r_{\rm D}$. A somewhat more favorable estimate results from the argument that it should actually suffice when ξ becomes large enough such that the distinct condensates form a percolating cluster throughout the sample; the condition for cooperative behavior then becomes $\xi \approx (n_c)^{1/d} r_{\rm D}$, where n_c denotes the percolation threshold.

In the following we give a more precise estimate $T_{\rm ord}$, in order to see if it may still be considerably above the transition temperature of the pure system T_c^0. Our strategy is to calculate the free–energy difference ΔF between the following two configurations in a two–defect system below the temperature where localized clusters may form in two different orientations: (i) both order parameter condensates oriented in the same direction, and (ii) opposite condensate orientations. The ensemble of localized clusters can then be effectively mapped onto an Ising system, with ΔF assuming the role of the exchange coupling. The critical temperature is now readily estimated as $k_{\rm B}T_{\rm ord} \approx \Delta F/a_0^3$ (a_0^3 is the volume of the elementary cell). We emphasize that we shall restrict ourselves to an isotropic system here, and consider the general case of an order parameter φ described by the usual Ginzburg–Landau expansion of the free energy, which rather corresponds to the case of distortive structural transitions, as studied in Ref. [8]. However, the qualitative behavior is expected to be very similar for the anisotropic elastic phase transitions.

Using the continuum representation, the free energy for a system in three dimensions with a single defect in the origin reads [3]

$$F = \int d^3r \left([a-\phi(\mathbf{r})]\varphi(\mathbf{r})^2 + c[\nabla\varphi(\mathbf{r})]^2 + \frac{d}{2}\varphi(\mathbf{r})^4 \right) \ , \tag{5.1}$$

where $\phi(\mathbf{r})$ is the positive δ function defect potential with strength $U = a_0^3\lambda$. The stationarity equation then becomes

$$c\nabla^2\varphi(\mathbf{r}) = [a-\phi(\mathbf{r})]\varphi(\mathbf{r}) + d\varphi(\mathbf{r})^3 \ , \tag{5.2}$$

which for $a > 0$ may be approximately solved by

$$r > R: \qquad \varphi(r) \approx \frac{\varphi_0 e^{r/\xi}}{1 + r e^{2r/\xi}/\xi} \approx \varphi_0 \frac{e^{-r/\xi}}{r/\xi} \tag{5.3}$$

$$r < R: \qquad \varphi(r) \approx \varphi_0 \left(1 - \frac{3r^2}{2\xi^2} \right) \ , \tag{5.4}$$

where $\xi = \sqrt{c/a}$ is the correlation length of the pure system for $T > T_c^0$, $\varphi_0^2 \approx (4\pi R^3\lambda/3 - 10a)/d$, and $R^3\lambda = 120\pi c^3(U_m^{-1} - U^{-1})^2$, with $U_m = 2\pi c a_0$ denoting the minimum defect strength required for the local order parameter condensation to occur.

Using these results, we can proceed towards the two–defect system with $\phi(\mathbf{r}) = U\delta(x)\delta(y)[\delta(z - r_{\rm D}/2) + \delta(z + r_{\rm D}/2)]$ by a simple linear superposition ansatz; i.e., we shall evaluate the free energy difference between the states

$$\varphi_\pm = \varphi(x,y,z - r_{\rm D}/2) \pm \varphi(x,y,z + r_{\rm D}/2) \ . \tag{5.5}$$

By inserting into Eq. (5.1) one readily finds the defect contribution

$$\Delta F_{\rm D} \approx -8U\varphi_0^2(\xi/r_{\rm D})e^{-r_{\rm D}/\xi} \ , \tag{5.6}$$

as well as the linear overlap integral (conveniently evaluated using elliptical coordinates)

$$\Delta F_{\rm lin} \approx 16\pi c\varphi_0^2\xi e^{-r_{\rm D}/\xi} \ ; \tag{5.7}$$

the nonlinear overlap integral turns out to be of order $e^{-2r_{\rm D}/\xi}$ and can thus be neglected for $\xi \leq r_{\rm D}$, when compared to the previous terms. Hence we find for the required free–energy difference

$$\Delta F \approx 16\pi c\varphi_0^2\xi e^{-r_{\rm D}/\xi}\left(1-\frac{U}{2\pi c r_{\rm D}}\right) \ ; \tag{5.8}$$

using the above numerical values, we see that the defect contribution can in fact be neglected here.

Hence we arrive at our final estimate for the cluster ordering temperature, which we identify with the "true" defect–induced transition temperature

$$k_{\rm B}T_{\rm ord} \approx 16\pi a\varphi_0^2(\xi/a_0)^3 e^{-r_{\rm D}/\xi} \ . \tag{5.9}$$

This expression may be cast into a somewhat more explicit form by observing that the average defect separation can be written as $r_{\rm D} = a_0 n_{\rm D}^{-1/3}$; thus the required defect concentration for the transition to occur at a certain value $T = T_{\rm ord}$ becomes

$$n_{\rm D} = \left(\frac{\xi_c}{a_0}\ln\left[\frac{16\pi a_c\phi_0^2}{k_{\rm B}T_{\rm ord}}\left(\frac{\xi_c}{a_0}\right)^3\right]\right)^{-3} \ , \tag{5.10}$$

from which $T_{\rm ord}$ as function of $n_{\rm D}$ may be inferred by inversion [$\xi_c = \sqrt{c/a_c}$, $a_c = a'(T_{\rm ord} - T_c^0)$]. The result is depicted in Fig.7. It can be seen that the calculated cluster ordering temperature may indeed be considerably above the phase transition temperature of the pure system $T_c^0 = 45$K, however, much larger impurity concentrations $n_{\rm D}$ are required than in the previous mean–field analysis.

For the anisotropic elastic systems discussed in the bulk of this paper, fluctuations will be even less important. We conclude this section with the remark that the upper critical dimension as function of the dimension m of the soft sector was found to be [14]

$$d_c(m) = 2 + \frac{m}{2} \ ; \tag{5.11}$$

thus in three dimensions mean–field theory yields exact results for a system with a one–dimensional soft sector, while for the case of a two–dimensional soft sector merely logarithmic corrections are to be expected.

VI. EXTENDED DISORDER: LINE AND PLANAR DEFECTS

We now return to the case of elastic phase transitions, and address the question of the influence of extended defects in contrast to the previously treated point disorder. Our system now contains randomly placed, but parallel linear or planar defects; the accordingly modified correlated defect potential (compare Eq. 2.3), reads in the case of line disorder

$$\phi(\mathbf{r}) = U\sum_{i_{\rm D}=1}^{N_{\rm D}} \delta(x-x_{i_{\rm D}})\delta(y-y_{i_{\rm D}}) \ , \tag{6.1}$$

where x, y, z are the components of $\mathbf{r}$, and z denotes the direction parallel to the lines; $i_{\rm D}$ labels the $N_{\rm D}$ line defects. The defect potential for planar defects is defined analogously, namely for planes normal to the x direction

$$\phi(\mathbf{r}) = U\sum_{i_{\rm D}=1}^{N_{\rm D}} \delta(x-x_{i_{\rm D}}) \ , \tag{6.2}$$

With these definitions the same calculations as before may be performed, and it becomes obvious that the former integrals reduce to integrals over the $\mathbf{k}$ vectors perpendicular to the defects. One gets qualitatively the same results as in the case of point defects.

In order to compare the effect of the different kinds of defects, we have calculated the order parameter in all three cases (points, lines, and planes) for the same defect strenght and the same defect concentration (i.e., the extended defects are viewed as correlated accumulations of point defects with the total number of – pointlike – defects held fixed). Therefore, the resulting differences solely originate in the different disorder dimensionality. The one–dimensional soft sector was taken to be perpendicular to the defects in order to provide a meaningful comparison. The result is depicted in Fig. 8; it can be seen that the effect of the defects is not a monotonous function of their dimensionality, but depends on the strength of two competing effects. On the one hand, when the temperature is lowered towards the phase transition temperature and the correlation length ξ grows accordingly, the order parameter cluster around a d'–dimensional defect grows proportional to $\xi^{d-d'}$. This effect renders low–dimensional defects more effective in influencing bulk properties. On the other hand, the system has a finite stiffness, characterized by the parameter c; and as a system with uncorrelated defects is more inhomogeneous than one with the identical amount of correlated disorder, this effect favors high–dimensional defects, because then the system stiffness can be more easily overcome by the joint action of neighboring defects. With the specific numerical values we have used, the line defects have only a tiny effect on the order parameter curve in comparison with the point defects. The effect of the planar defects lies in between. We emphasize that this scenario could be different for other values of the stiffness parameter c. Finally, we remark that if one performs the above calculations for a system with extended defects, where the soft sector is not perpendicular to the defects, additional angle dependences ensue, and one has to add an additional term of the form cq^4

to the functional (2.2), in order to correctly account for the stiffness, which tends to prevent the building–up of order parameter clusters.

VII. SUMMARY AND DISCUSSION

In this paper we have studied the influence of point and extended defects on a d–dimensional elastic system with an m–dimensional soft sector undergoing an elastic phase transition of second order. We have calculated the phonon–phonon correlation function in the high–temperature phase. At a certain temperature $T_c(n_{\rm D}) \gg T_c^0$, an instability marking a defect–induced phase transition may emerge, if the defect potentials are sufficiently strong. Above $T_c(n_{\rm D})$ a dynamical central peak emerges in the phonon correlation function, whose intensity grows as the temperature is lowered towards $T_c(n_{\rm D})$. Contrary to the case of distortive phase transitions [8], the maximum of the central peak is exactly at $\omega = 0$ for all temperatures and not at small but finite frequencies [7]. This, however, does not imply that the acoustic impurity modes are localized; at least for a simplifying one–dimensional single–defect model no additional localized impurity modes appear, but the defect rather causes a localized vibrational contribution to the propagating scattering states; for the long–wavelength phonons this quasi–resonant vibration then condenses at $T_c(n_{\rm D})$ and forms the local order parameter clusters [7]. The dynamical central peak may be regarded as precursor of this phase transition; its height also depends on the angle between the external wave vector $\mathbf{k}$ and the soft sector. The smaller this angle, the more pronounced is the central peak.

In the low–temperature phase $T < T_c(n_{\rm D})$, where a finite, and be it ever so small, order parameter exists, we have used a self–consistent mean–field calculation in order to calculate the average order parameter, the free energy and specific heat, and the phonon correlation function. The order parameter sets in continuously at $T_c(n_{\rm D})$, remains very small in the temperature range between $T_c(n_{\rm D})$ and T_c^0, and reaches appreciable values only near T_c^0. In this way the order parameter curve resembles a somewhat rounded curve of the pure system. Analogously, the temperature dependence of the specific heat looks like the corresponding smeared–out curve for the pure system. The jump at T_c^0 is rounded, and a minute jump at $T_c(n_{\rm D})$ appears. Thus the phase transition of the perturbed system no longer occurs at T_c^0 but at $T_c(n_{\rm D})$. However, the phase transition temperature T_c^0 of the pure system remains important, as the remnants of the pure transitions induce marked, but rounded maxima in quantities like the order parameter susceptibility or the specific heat near T_c^0.

Having thus determined the order parameter, we were able to calculate the phonon correlation function in the ordered phase. The dynamical central peak disappears again as the temperature is lowered below $T_c(n_{\rm D})$. The dependence of the central peak on the angle between the momentum transfer vector $\mathbf{k}$ and the soft sector is very similar as above $T_c(n_{\rm D})$. The density–density correlation function determining the cross section for scattering experiments consists of three terms: first, the term describing elastic Bragg scattering, second, a term corresponding to Huang scattering caused by the spatially inhomogeneous order parameter configuration; this term yields a contribution to elastic scattering, leading to a static central peak with finite k width. The third term finally describes inelastic scattering and has been discussed along with the phonon correlation function.

We have also discussed the validity of our mean–field approach and provided an estimate (in the isotropic case) for the "true" precursor T_c, defined as the cluster ordering temperature $T_{\rm ord}$, which has to be distinguished from the temperature $T_c(n_{\rm D})$ where localized, but fluctuating order parameter clusters appear. Only below $T_{\rm ord}$, the previously independent ordered regions form a collective state leading to a non–zero average order parameter. Generally, cooperative behavior of the defects is to be expected when the correlation length of the pure system ξ becomes of the order of the mean defect separation $r_{\rm D}$. Although the ensuing cluster ordering temperature is considerably lower than $T_c(n_{\rm D})$, the qualitative features of the present theory should remain largely unaffected, provided $T_c(n_{\rm D})$ is replaced by $T_{\rm ord}$; i.e., the mean order parameter appears rounded near T_c^0, while static order parameter susceptibility and the specific heat display a strong but broadened maximum there. Furthermore, in the anisotropic systems under consideration here, fluctuations may actually be suppressed, rendering mean–field theory more reliable. Finally, the time scale of the order parameter condensate fluctuations will diverge $\propto (T - T_{\rm ord})^{-1}$ upon approaching $T_{\rm ord}$, which in experiment would eventually render them indistinguishable from static inhomogeneities, leading to quasi–elastic Bragg and Huang scattering peaks. We have also investigated the case of parallel extended defects (lines and planes), and found essentially the same features [21].

These considerations led us to the qualitative phase diagram displayed in Fig.7. For very tiny disorder concentrations, the picture of isolated defects applies. Although preordered clusters may form considerably above T_c^0, the ensuing condensates fluctuate independently and do not form a state with nonzero average order parameter. The cluster reorientation rate will become very low as T_c^0 is approached, and coupling of these slow modes to the soft (acoustic) phonons will then lead to a dynamical central peak, see Ref. [1]. For higher, but still small defect concentrations, the clusters emerging at $T_c(n_{rmD})$ will form a state with preordered defect regions and finite, but small average order parameter below $T_{\rm ord}$. This phase transition leads to discontinuities in thermodynamic quantities, like the specific heat or the static susceptibility, which are, however, probably unnoticeably small in experiment. On the other hand,

upon approaching T_c^0, the phase transition temperature of the pure crystal, the bulk system orders; due to the influence of the preordered defect regions, the transition temperature will be slightly higher than T_c^0, and the formerly sharp singularities of the mean order parameter, specific heat, and static susceptibility appear characteristically rounded. The above described theory applies precisely to this concentration range (for very strong disorder the single–site approximation breaks down). The central peak phenomenon is thus explained by a combination of elastic Bragg peaks of the low–temperature phase and static Huang scattering with finite width in q space.

However, a different scenario is also conceivable, namely that as the cluster reorientation times become very long, the different, still independent condensates freeze in with spatially fluctuating orientations. The ensuing configuration would constitute a metastable state which is separated from the true ground state by high free energy barriers Δ. The typical flip rate would then be proportional to $\exp(-\Delta/k_{\rm B}T)$; therefore, at low temperatures the true thermodynamic ground state may not be reached. In the spirit of the discussion in Sec.V one could possibly map this problem onto a random–field Ising model (for recent reviews, see, e.g. Ref. [22]), the lower critical dimension of which is $d_l = 2$, and therefore long–range order is not destroyed in three dimensions.

At last, we would like to contrast our picture with that of "glassy" systems. Although some of the features of the dynamical structure factor in glasses are at least qualitatively similar, e.g., an elastic peak with finite q width appears, and the static susceptibility and specific heat may display characteristically rounded and broadened maxima, there are important differences. First, the order parameter of the pure crystal $\bar{\nu}$ would not constitute an appropriate order parameter for such a disordered, glassy system. Second, the character of the phase transition should be entirely different, and in fact lead to experimentally distinguishable behavior. The scenario described here is a genuine second–order phase transition, though induced by disorder (which locally softens the system); i.e.: critical phenomena are confined to regions very close to $T_c(n_{\rm D})$ (or $T_{\rm ord}$), and to wave vectors in the soft sector with $\mathbf{p} \approx 0$. The freezing–in into a glassy state, on the other hand, would have to be described by an ergodicity–breaking (Edwards–Anderson) order parameter, and should actually be rather insensitive to k. Such a glass instability occurs, e.g., in orientational glasses [23], and possibly in relaxor ferroelectrics [24]. We finally remark that for the case of first–order martensitic transformations, a model with disorder of the random T_c type has been proposed, which can then be mapped onto a spin glass, and the ensuing glassy features were suggested to explain the prominent tweed microstructure found in these materials, as well as the central peak phenomenon there [25].

ACKNOWLEDGMENTS

U.C.T. acknowledges support from the Deutsche Forschungsgemeinschaft (DFG) under Contract Ta. 177/1-2.

* Present address: University of Oxford, Department of Physics – Theoretical Physics, 1 Keble Road, Oxford OX1 3NP, U.K.

[1] F. Schwabl, in: *Anharmonic Lattices, Structural Transitions, and Melting*, ed. T. Riste (Noordhoff, Leiden, 1974); p. 87; R. Folk and F. Schwabl, Solid State Comm. **15**, 937 (1974); F. Schwabl, in: *Ferroelektrische Phasenübergänge, 3. Frühjahrsschule "Ferroelektrizität"*, ed. W. Windsch (Martin–Luther-Universität Halle, 1975), p. 47.

[2] B.I. Halperin and C.M. Varma, Phys. Rev. B **14**, 4030 (1976).

[3] H. Schmidt and F. Schwabl, Phys. Lett. **61 A**, 476 (1977); in: *Proceedings of the International Conference on Lattice Dynamics*, ed. M. Balkanski (Flammarion Sciences, Paris, 1977), p. 748; Z. Phys. B **30**, 197 (1978).

[4] K.H. Höck and H. Thomas, Z. Phys. B **27**, 267 (1977); K.H. Höck, R. Schäfer, and H. Thomas, Z. Phys. B **36**, 151 (1979).

[5] L. Sasvári and F. Schwabl, Z. Phys. B **46**, 269 (1982).

[6] K.H. Weyrich and R. Siems, Ferroelectrics **55**, 333 (1984); B. Wiesen, K.H. Weyrich, and R. Siems, Phys. Rev. B **36**, 3175 (1987); Ferroelectrics **79**, 69 (1988).

[7] F. Schwabl and U.C. Täuber, Phase Transitions **34**, 69 (1991).

[8] F. Schwabl and U.C. Täuber, Phys. Rev. B **43**, 11112 (1991).

[9] T. Riste, E.J. Samuelsen, K. Otnes, and J. Feder, Solid State Comm. **9**, 1455 (1971); S.M. Shapiro, J.D. Axe, G. Shirane, and T. Riste, Phys. Rev. B **6**, 4332 (1972).

[10] G. Shirane and J.D. Axe, Phys. Rev. Lett. **27**, 1803 (1971).

[11] K.A. Müller, in: *Dynamical Critical Phenomena and Related Topics*, ed. C.P. Enz (Springer–Verlag, Berlin, 1979), p. 210.

[12] P.A. Fleury and K.B. Lyons, in: *Light Scattering Near Phase Transitions*, ed. H.Z. Cummins and A.P. Levanyuk (North Holland, Amsterdam, 1982), p. 449.

[13] A.D. Bruce and R.A. Cowley, *Structural Phase Transitions*, (Taylor and Francis, London, 1981) [Adv. Phys. **29**, 1 (1980)].

[14] R. Folk, H. Iro, and F. Schwabl, Phys. Lett. **57 A**, 112 (1976); Z. Phys. B **25**, 69 (1976).

[15] R.A. Cowley, Phys. Rev. B **13**, 4877 (1976).

[16] R. Folk, H. Iro, and F. Schwabl, Phys. Rev. B **20**, 1229 (1979); in: *Proceedings of the International Conference on Lattice Dynamics*, ed. M. Balkanski (Flammarion Sci-

ences, Paris, 1977), p. 702; F. Schwabl, J. Stat. Phys. **39**, 719 (1985).
[17] J.S. Langer, J. Math. Phys. **2**, 584 (1961).
[18] R.J. Elliott, J.A. Krumhansl, and P.L. Leath, Rev. Mod. Phys. **46**, 465 (1974).
[19] J.D. Axe and G. Shirane, Phys. Rev. B **8**, 1965 (1973).
[20] W. Rehwald, Phys. Lett. **27 A**, 287 (1968).
[21] M. Bulenda, Diploma thesis, Technische Universit"at M"unchen 1993 (unpublished).
[22] T. Nattermann and J. Villain, Phase Transitions **11**, 5 (1988); T. Nattermann and P. Rujan, Int. J. Mod. Phys. **3**, 1597 (1989).
[23] K.H. Michel, Z. Phys. B **68**, 259 (1987); C. Bostoen and K.H. Michel, Phys. Rev. B **43**, 4415 (1991).
[24] D. Viehland, S.J. Jang, L.E. Cross, and M. Wuttig, Phys. Rev. B **46**, 8003 (1992).
[25] S. Kartha, T. Castán, J.A. Krumhansl, and J.P. Sethna, Phys. Rev. Lett. **67**, 3630 (1991); J.P. Sethna, S. Kartha, T. Castán, and J.A. Krumhansl, Phys. Scr. **T42**, 214 (1992); S. Kartha, J.A. Krumhansl, J.P. Sethna, and L.K. Wickham, Phys. Rev. B **52**, 803 (1995).

TABLE I. Ginzburg-Landau parameters, as used in the figures, if not specified otherwise $[a = a'(T - T_c^0)]$.

$T_c^0 = 45$ K
$a' = 1.0771 \cdot 10^{-12}$erg K^{-1}
$d = 1.1363 \cdot 10^{-8}$erg
$M = 1.314 \cdot 10^{-21}$g
$b = 1.570 \cdot 10^{-10}$erg
$c = 5 \cdot 10^{-26}$erg cm^2
$N/V = 6.751 \cdot 10^{21}$cm^{-3}
$\lambda = 3.0994 \cdot 10^{-11}$erg
$D = \tilde{D} = 1 \cdot 10^{-3}$cm^{2}s^{-1}
$k = \zeta \cdot \sqrt{2} \cdot a^*$
$a^* = 2\pi/a_0 = 1.189 \cdot 10^8$cm^{-1}
$T_c(n_{\rm D}) = 65$K
$n_{\rm D} = 1 \cdot 10^{-5}$
$\lambda = 3.0994 \cdot 10^{-11}$erg

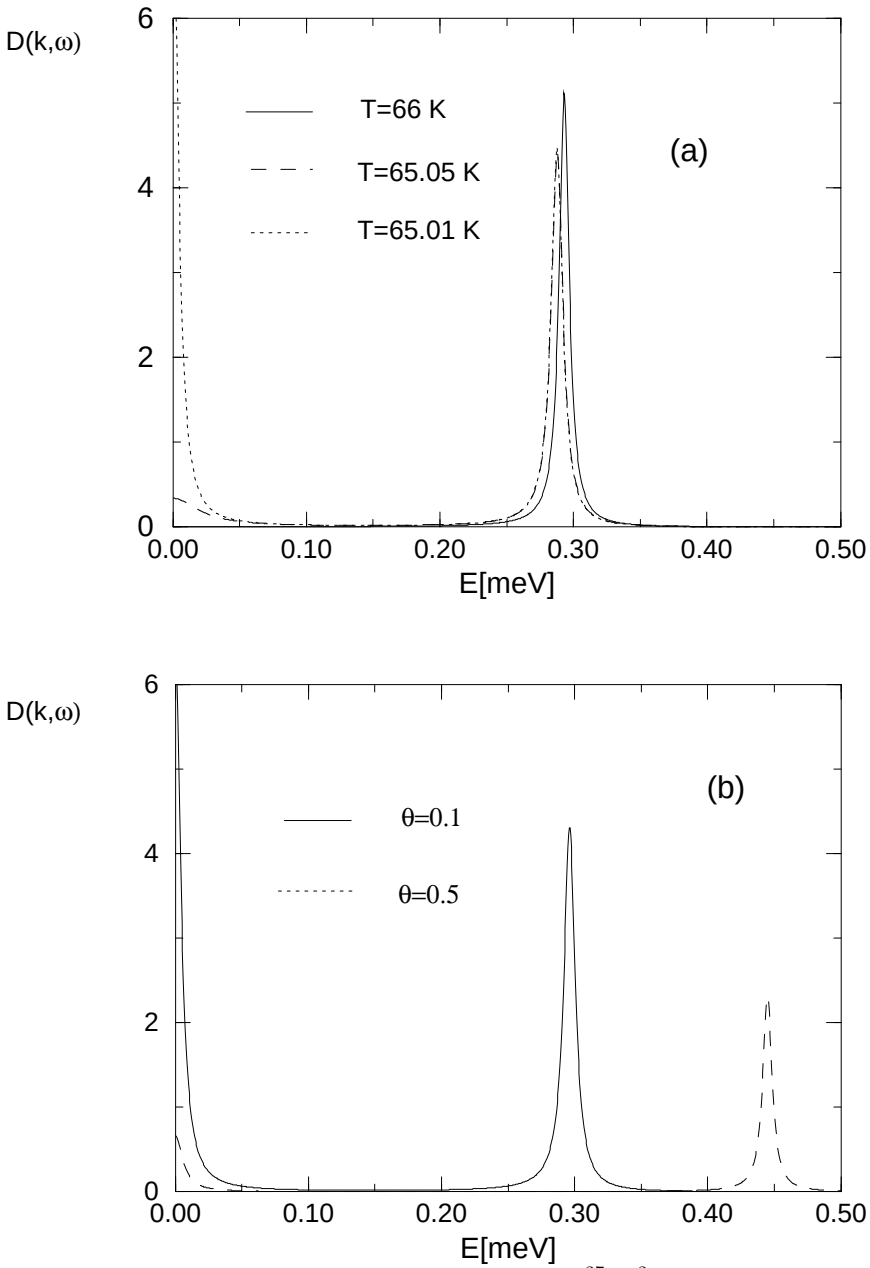

FIG. 1. Phonon correlation function $D(\mathbf{k},\omega) = 2k_{\rm B}T{\rm ImG}(\mathbf{k},\omega)/\omega$ [in $10^{-27}{\rm cm}^2{\rm s}$] vs. phonon energy [in meV] for different temperatures and fixed angle $\theta = 0$ (a), and for fixed temperature $T = 65.01$ K with different angles θ (b); $\zeta = ka_0/2^{3/2}\pi = 0.02$ was used.

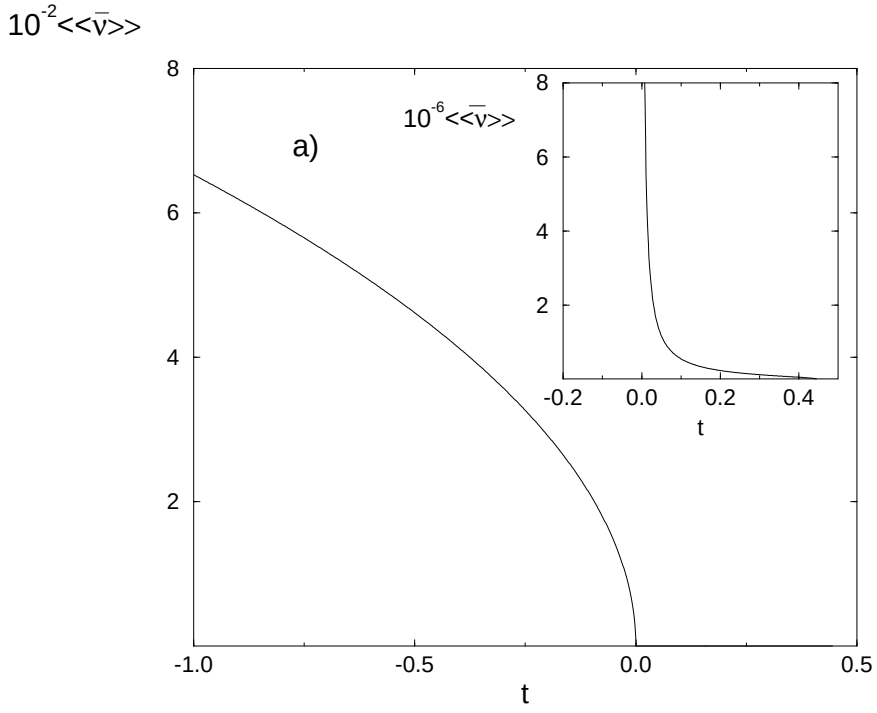

FIG. 2. Average order parameter $\langle\langle\bar{\nu}\rangle\rangle$ vs. reduced temperature t for $n_{\rm D} = 10^{-5}$, $\lambda = 3.0994 \cdot 10^{-11}$erg (a), and $n_{\rm D} = 10^{-3}$, $\lambda = 3.0949 \cdot 10^{-11}$erg (b). The temperature range near $t_c(n_{\rm D}) = 0.444$ is displayed in the insets. Note the different scales of the two insets; the disorder strength was adjusted to yield the same $T_c(n_{\rm D})$ in both cases (a) and (b).

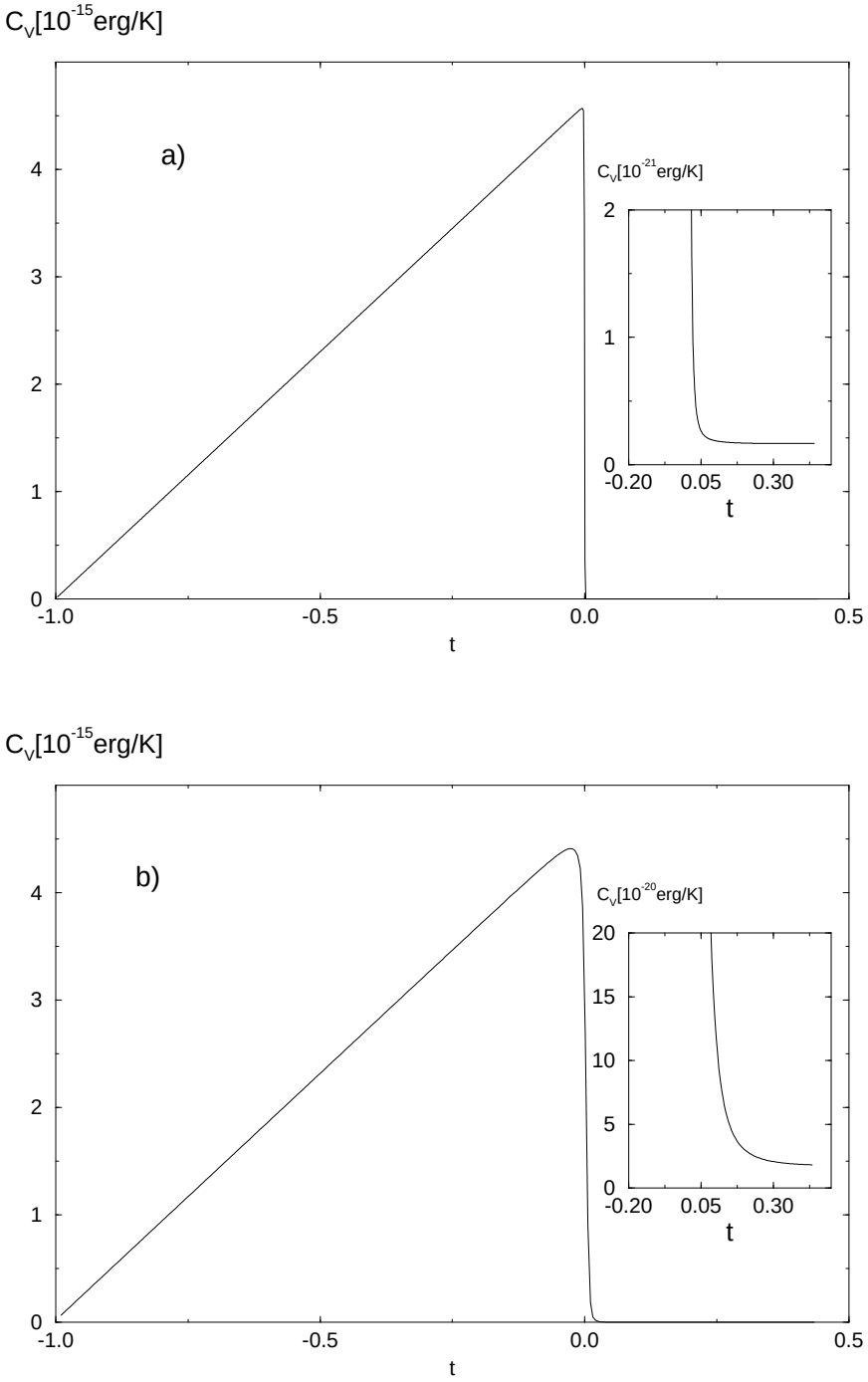

FIG. 3. Specific heat C_v vs. reduced temperature t for $n_{\rm D} = 10^{-5}$ (a) and $n_{\rm D} = 10^{-3}$ (b). The defect–induced temperature has been adjusted to $t_c(n_{\rm D}) = 0.444$ in both cases by changing the defect potential strength accordingly, see Fig.2. The temperature range near $t_c(n_{\rm D})$ is displayed in the insets; note the different scales.

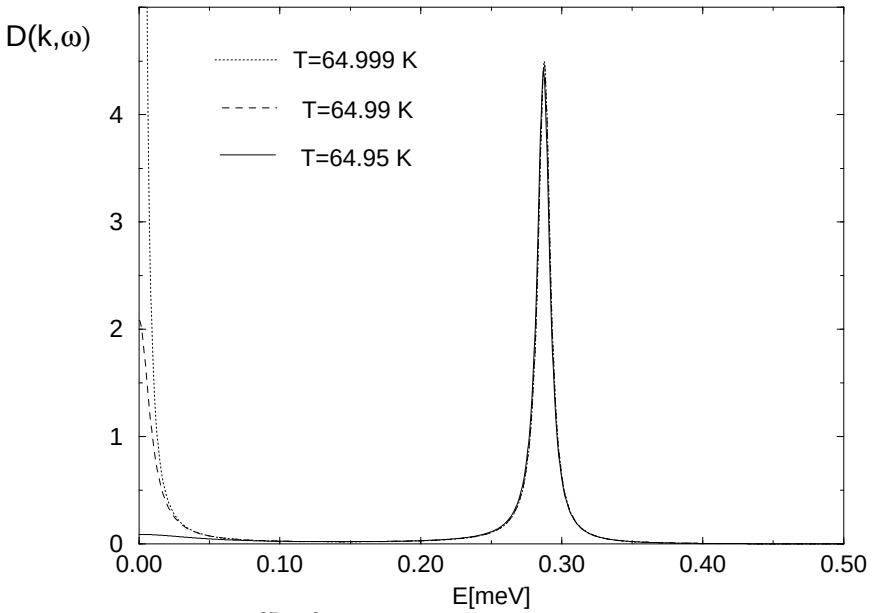

FIG. 4. Phonon correlation function [in $10^{-27}\mathrm{cm}^2\mathrm{s}$] vs. phonon energy in [meV] for different temperatures below $T_c(n_\mathrm{D})$ at fixed angle $\theta = 0$. As before, $t_c(n_\mathrm{D}) = 0.444$, and $\zeta = ka_0/2^{3/2}\pi = 0.02$ was used.

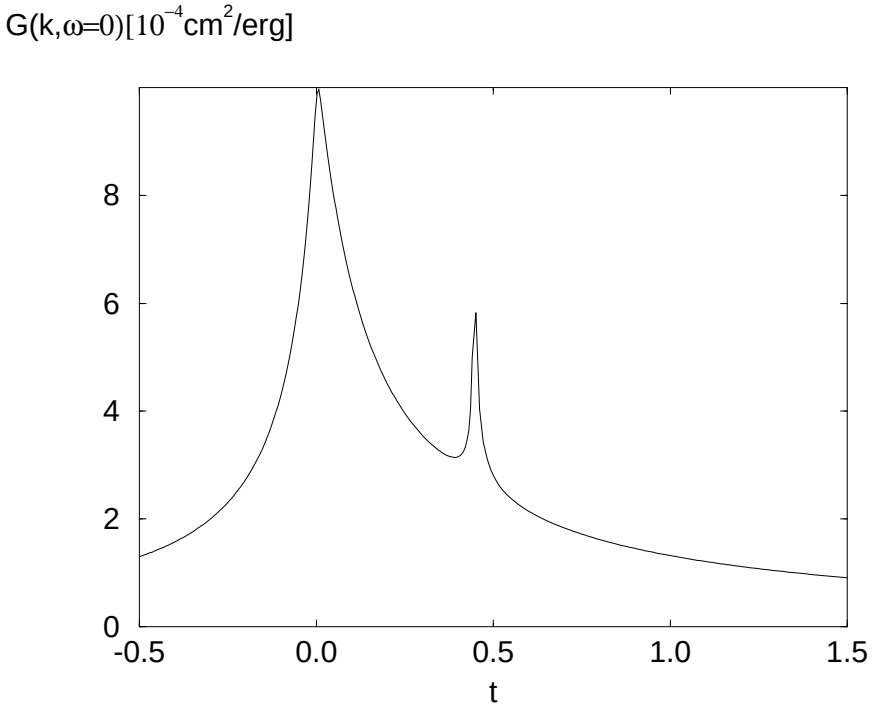

FIG. 5. Static phonon susceptibility (inverse elastic constant) $G(\mathbf{k})$ [in $10^{-4}\mathrm{cm}^2\mathrm{erg}^{-1}$] vs. temperature at fixed angle $\theta = 0$. 9 $t_c(n_\mathrm{D}) = 0.444$, $\zeta = ka_0/2^{3/2}\pi = 0.07$.

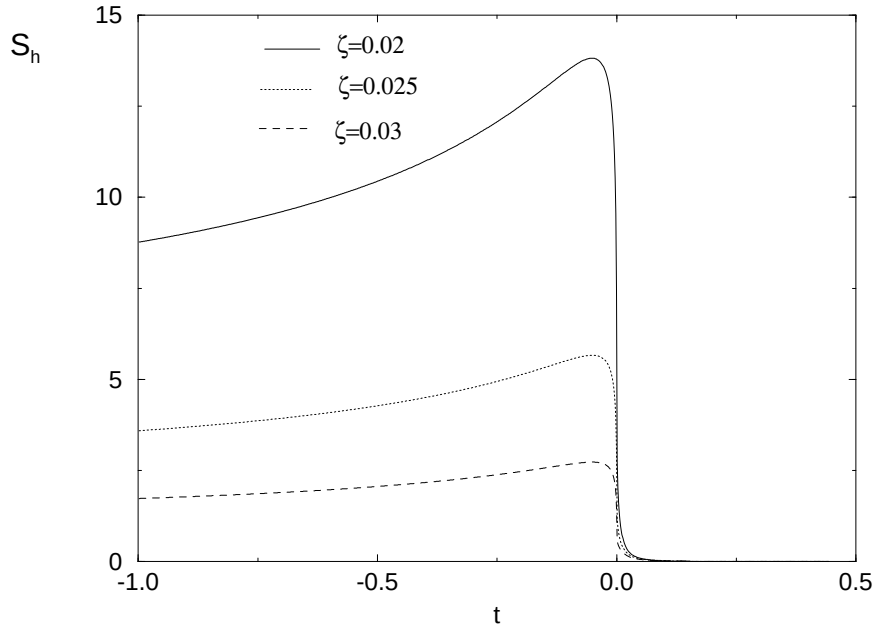

FIG. 6. The term $\langle\langle\bar{\nu}\rangle\rangle^2\tilde{G}_0(\mathbf{k})^2(a+dA^2)^2$, denoted by S_h [in units 10^{-11}] vs. reduced temperature t for different wavevectors. The wave vector $\mathbf{k}$ lies in the soft sector.

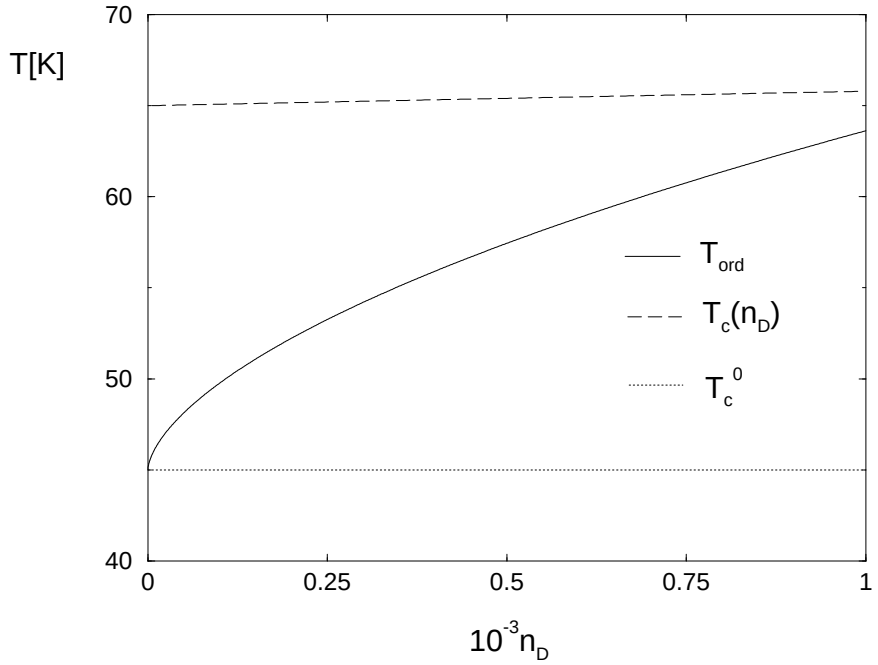

FIG. 7. Cluster ordering (precursor) temperature $T_{\rm ord}$ and mean–field (local) transition temperature $T_c(n_{\rm D})$ [in K] as function of the defect concentration $n_{\rm D}$; the numerical values of Table I were used here.

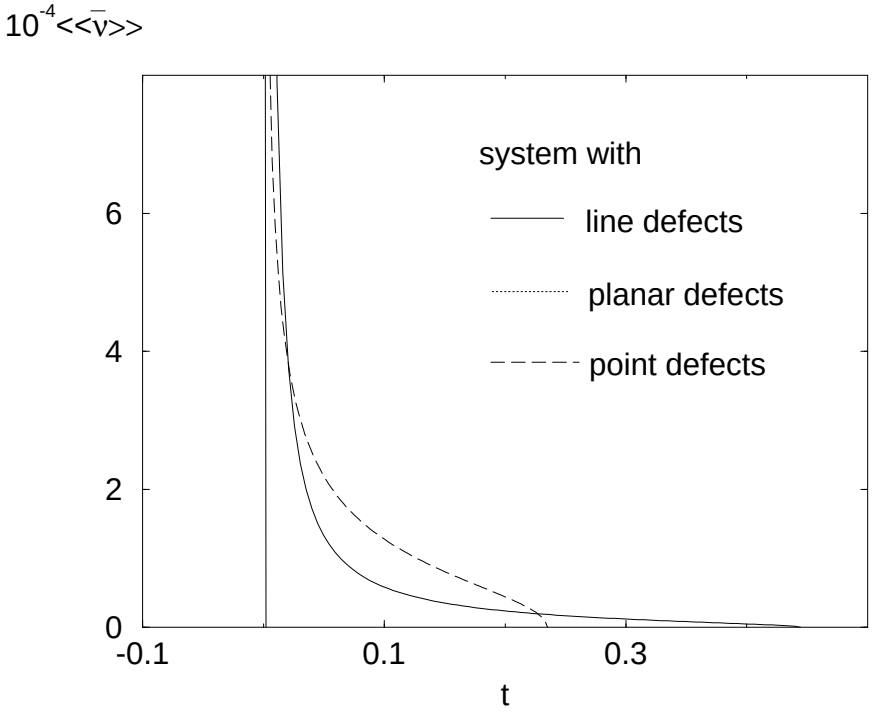

FIG. 8. Order parameter vs. reduced temperature for systems with different types of defects; the numerical values of Table I and $n_{\rm D} = 10^{-3}$ were used here.